Peroxisomal and mitochondrial status of two murine oligodendrocytic cell lines (158N, 158JP): potential models for the study of peroxisomal disorders associated with dysmyelination processes.

Mauhamad Baarine, Kevin Ragot, Emmanuelle C. Genin, Hammam El Hajj, Doriane Trompier, Pierre Andreoletti, M Said Ghandour, Franck Ménétrier, Mustapha Cherkaoui-Malki, Stéphane Savary, et al.

Peroxisomal and Mitochondrial Status of Two Murine Oligodendrocytic Cell Lines (158N, 158JP): Potential Models for the Study of Peroxisomal Disorders Associated with Dysmyelination Processes

Running title: Peroxisomal and Mitochondrial Status of Two Differentiated Murine Oligodendrocytic Cell Lines (158N, 158JP)

MAUHAMAD BAARINE,[1,2] **KEVIN RAGOT,**[1,2] **EMMANUELLE C. GENIN,**[1,2] **HAMMAM EL HAJJ,** [1,2] **DORIANE TROMPIER,**[1,2] **PIERRE ANDREOLETTI,**[1,2] **SAID GHANDOUR,**[3] **FRANCK MENETRIER,**[4] **MUSTAPHA CHERKAOUI-MALKI,**[1,2] **STEPHANE SAVARY,**[1, 2] **GERARD LIZARD**[1, 2*]

[1] Centre de Recherche INSERM 866, Dijon, F-21000, France.

[2] Université de Bourgogne, Faculté des Sciences Gabriel, Centre de Recherche Lipides, Nutrition, Cancer-Laboratoire de Biochimie Métabolique et Nutritionnelle (LBMN), GDR CNRS 2583, Dijon, 21000, France.

[3] Biopathologie et Imagerie de la Myéline, UMR 7191 CNRS / ULP Laboratoire d'Imagerie et de Neurosciences Cognitives (LINC), Université Louis Pasteur, Faculté de Médecine, 11 rue Humann, 67085 Strasbourg, France.

[4] IFR Santé / STIC Inserm, Centre de Microscopie Préparative Appliqué à la Biologie et à la Médecine, 7 Bd Jeanne d'Arc, 21033 Dijon Cedex, France.

[*]**Correspondence to** Dr. Gérard Lizard, CRInserm 866, Faculté des Sciences Gabriel, 6 Bd Gabriel, 21000 Dijon, France; Phone: +33 380 39 62 56; Fax: +33 380 39 62 50

E.mail: Gerard.Lizard@u-bourgogne.fr

ABSTRACT

In some neurodegenerative disorders (leukodystrophies) characterized by myelin alterations, the defect of peroxisomal functions on myelin-producing cells (oligodendrocytes) are poorly understood. The development of *in vitro* models is fundamental to understanding the physiopathogenesis of these diseases. We characterized two immortalized murine oligodendrocyte cell lines: a normal (158N) and a jimpy (158JP) cell line mutated for the proteolipid protein PLP/DM20. Fluorescence microscopy, flow cytometry, and Western blotting analysis allow to identify major myelin proteins (PLP colocalizing with mitochondria; MBP), oligodendrocyte (CNPase, MOG), and peroxisomal markers (ALDP, PMP70, ACOX1, L-PBE, catalase). Using electron microscopy, peroxisomes were identified in the two cell lines. Gene expression (*Abcd1*, *Abcd2*, *Abcd3*, *Acox1*) involved in peroxisomal transport or β-oxidation of fatty acids was evaluated using quantitative PCR. 4-phenylbutyrate (4-PBA) treatment increases expression of ACOX1, L-PBE, PLP, MOG, and CNPase, mainly in 158N cells. In both cell lines, 4-PBA induced ACOX1 and catalase activities while only *Abcd2* gene was up-regulated in 158JP. Moreover, the higher mitochondrial activity and content observed in 158JP were associated with higher glutathione content and increased basal production of reactive oxygen species revealing different redox statuses. Altogether, 158N and 158JP cells will permit studying the relationships between peroxisomal defects, mitochondrial activity, and oligodendrocyte functions.

KEY WORDS murine oligodendrocytes; peroxisome; mitochondria; myelin

INTRODUCTION

Peroxisomes are single cell membrane organelles ensuring essential cellular functions, particularly in lipid metabolism (Wanders and Waterham, 2006a; Schrader and Fahimi, 2008). These organelles are involved in the β-oxidation process of long- and very-long-chain fatty acids (LCFA, VLCFA), branched-chain fatty acids, unsaturated fatty acids, and dicarboxylic acids (Nguyen et al., 2008). They participate in the α-oxidation of phytanic acid, the biosynthesis of bile acids, and the degradation of leukotrienes (Schrader and Fahimi, 2008). They are also involved in the synthesis of specific fatty acids, such as docosahexaenoic acid (DHA, C22:6 n-3), which are essential for the brain and the retina, as well as the synthesis of plasmalogens, which play essential roles in the growth of neural cells and are important components of myelin, a complex of lipids and proteins (30% proteins, 70% lipids) (Harauz et al., 2004; Hörster et al., 2005). In the central nervous system (CNS), the myelin sheath is formed by membranes that extend from oligodendrocytes that wrap concentrically around nerve fibres, thereby insulating them and facilitating rapid transmission of nerve impulses (Harauz et al., 2004). Consequently, alteration of peroxisomal functions induces lipid modifications that are detrimental for the development and functions of the nervous system.

Besides peroxisome biogenesis disorders (Schrader and Sahimi, 2008), several disorders associated with a single defect in the β-oxidation process have been described. They are characterized by either developmental or degenerative pathologies, in particular in the central and peripheral nervous system (Wanders and Waterham, 2006a). These pathologies are usually characterized by a dysmyelination of the white matter belonging to the so-called leukodystrophies and are characterized by the accumulation of VLCFA in plasma and tissues due to an impaired β-oxidation in peroxisomes and/or increased elongation (Wanders and Waterham, 2006b). X-linked adrenoleukodystrophy (X-ALD, OMIM 300100), the most frequent leukodystrophy, affects either young boys (cerebral childhood ALD, CCALD, 40%

of the cases) leading to a vegetative state or death, or adults (adrenomyeloneuropathy, AMN, 50% of the cases). X-ALD is caused by mutations in the *ABCD1* gene located in Xq28 (Berger and Gartner, 2006; Kemp and Wanders, 2007) encoding a peroxisomal ATP-binding cassette (ABC) half-transporter called the adrenoleukodystrophy protein (ALDP), which participates in the entry of VLCFA-CoA into the peroxisome. CCALD is associated with a strong inflammatory reaction and iNOS induction in the CNS white matter (Paintlia et al., 2003). Pseudo-neonatal adrenoleukodystrophy (P-NALD, OMIM 264470), characterized by a generalized hypotonia and severe delayed motor development, is caused by mutations in the gene encoding the peroxisomal straight-chain acyl-CoA oxidase (ACOX1) located in 17q25. P-NALD is associated with an enzymatic deficiency of ACOX1, which catalyzes the first and rate-limiting step of straight-chain fatty acid β-oxidation (Poll-The et al., 1988; Jia et al., 2004).

Understanding the mechanism of dysmyelination in these disorders is a major challenge to further developing efficient treatments and/or improving the quality of life of these patients, particularly X-ALD patients. While the mice models deficient in ALDP or ACOX1 do not mimic the human pathologies since they do not develop alterations in the CNS (Forss-Petter et al., 1997), it has been reported that the selective absence of peroxisomes in oligodendrocytes in *CNP-Pex5* knockout mice causes progressive demyelination (Kassmann et al., 2007). Similarly, in *Nes-Pex5* knockout mice, a clear reduction in myelin fibres is observed (Hulshagen et al., 2008). Consequently, it is important to clarify the relationships between the peroxisomal deficiencies in oligodendrocytes, the VLCFA accumulation, and the dysmyelination process. Currently, several human and murine oligodendrocytic cell lines have been established, and those expressing major myelin proteins could constitute interesting biological models to study these relationships. However, most of these cell lines (human oligodendrial cell lines MOG, MO3.13, and KG-1C (Buntinx et al., 2003); clones JP1.1 and

JP1.2, obtained by immortalization of oligodendrocytes from jimpy mice with the temperature-sensitive SV40 large T antigen (Bongarzone et al., 1997); the mouse oligodendrocyte cell lines N20.1 and N19 obtained by immortalization of oligodendrocytes from normal mice (Verity et al., 1993)) present oligodendrocytic precursor phenotypes. Interestingly, two murine oligodendrocytic cell lines, 158N and 158JP, obtained by immortalization with the SV-40 large T antigen of oligodendrocytes from normal and jimpy mice, respectively, show phenotypes of well-differentiated oligodendrocytes (Feutz et al., 1995; Feutz et al., 2001; Ghandour et al., 2002). Jimpy mice are characterized by a single mutation (A-to-G) at the splice acceptor site of exon 5 of the proteolipid protein *PLP/DM20* gene, producing a deletion of the entire exon 5 and a translation frame shift of the mRNA, which results in a modified C-terminus in the jimpy proteolipid protein (PLP) and of its isoform DM20 (Macklin et al., 1987). The 158N and 158JP cells express the main markers of well-differentiated oligodendrocytes: carbonic anhydrase II (CAII), galactocerebroside, and the major myelin proteins, PLP and the myelin basic protein (MBP) known to account for 50% and 30% of myelin proteins, respectively (Harauz et al., 2004; Taylor et al., 2004). So, these cell lines could be suitable *in vitro* models to study the side effects resulting from an intracellular accumulation of VLCFA on the synthesis of major myelin proteins.

In order to define whether these cells can be useful to study the relationships between VLCFA accumulation, peroxisomal activity, and the expression of the major myelin proteins, we characterized their peroxisomal equipment by transmission electronic microscopy and analyzed the expression of oligodendrocytic and peroxisomal markers at the transcriptional and/or translational levels by various methods (fluorescence microscopy, flow cytometry, Western blotting, real-time PCR). We were interested in myelin proteins including PLP and MBP, in markers of differentiated oligodendrocytes (CNPase, myelin oligodendrocyte glycoprotein (MOG)), as well as in several peroxisomal markers (ALDP (ABCD1), ALDRP

(ABCD2) and PMP70 (ABCD3), peroxisomal bifunctional enzyme (L-PBE), acyl-CoA oxidase 1 (ACOX1), and catalase). Catalase and ACOX1 activities were also quantified by spectrophotometry and fluorimetry, respectively. Moreover, we tested the ability of 158N and 158JP cells to respond to 4-phenylbutyrate (4-PBA) known to induce peroxisome proliferation and peroxisomal genes (Gondcaille et al., 2005) and to be efficient in reducing VLCFA accumulation in the brain of *Abcd1*-null mice (Kemp et al., 1998). In addition, since the mitochondrial and redox status can be modified in the case of *ABCD1* deficiency and/or VLCFA accumulation (Hein et al., 2008; Fourcade et al., 2008), mitochondrial activity and content as well as redox status were measured by flow cytometry. Finally, since abnormal PLP expression leading to demyelination can modulate mitochondrial activity (Bongarzone et al., 2001), the interaction of PLP with mitochondria was investigated by laser scanning confocal microscopy.

MATERIALS AND METHODS

Reagents

Antibodies raised against MBP (ab53294), PLP (ab28486), and catalase (ab16771) were purchased from Abcam; PMP70 antibodies (71-8300) from Invitrogen; MOG antibodies (MAB2439) from R&D systems; CNPase antibodies (C5922) from Sigma. Antibodies against ACOX1 and L-peroxisomal bifunctional enzyme (L-PBE) have been described elsewhere (Huin et al., 2002), and were produced in the laboratory by Pr Cherkaoui-Malki. Antibodies raised against ALDP (serum 1664) were a generous gift from Pr Aubourg (INSERM, Paris, France) (Fouquet et al., 1997). The following dyes were used: Hoechst 33342 and H_2-DCFDA (Sigma Aldrich); dihydroethidium (DHE), nonylacridine orange (NAO), Mitotracker Red and *3,3*'-dihexyloxacarbocyanine iodide ($DiOC_6(3)$) (Molecular Probes/Invitrogen); monochlorobimane (MCB) (Biochemika). The Amplex Red catalase assay kit was from Invitrogen. The 4-PBA used was from Sigma-Aldrich.

Cells, cell cultures, and cell treatments

Murine oligodendrocytic cells 158N and 158JP (Feutz et al., 2001) were seeded at 5,000–10,000 cells/cm^2 either in 75-cm^2 culture flasks or in Petri dishes (100 mm in diameter) in Dulbecco's Modified Eagle Medium supplemented with 5% (v/v) heat inactivated foetal bovine serum (PAN™ Biotech GmbH)). Cells were incubated at 37°C in a wet atmosphere containing 5% CO_2. The conditions of treatment with 4-PBA were the following. After plating cells in culture flasks for 24 h, they were treated for 72 h with 2.5 mM of 4-PBA.

Transmission electron microscopy of peroxisomes and mitochondria

Transmission electron microscopy was used to visualize peroxisomes and mitochondria in 158N and 158JP cells cultured in the absence or in the presence of 4-PBA (2.5 mM, 72 h).

Hepatic sections of 9- to 10-week-old C57 Black/6 males were used as positive controls for peroxisomal analysis. For peroxisomal localization, cells and tissue sections were prepared as follows (Schrader et al., 1994). The samples were fixed for 1 h at 4°C in 2.5% (w/v) glutaraldehyde diluted in cacodylate buffer (0.1 M, pH 7.4), washed in cacodylate buffer (0.1 M, pH 7.4), incubated in the dark for 1 h at room temperature in Tris-HCl (0.05 M, pH 9.0) containing diaminobenzidine (DAB) (2.5 mg/ml) and H_2O_2 (10 µl/ml of a 3% solution), washed in cacodylate buffer (0.1 M, pH 7.4) for 5 min at room temperature, post-fixed in 1% (w/v) osmium tetroxide diluted in cacodylate sodium (0.1 M, pH 7.4) for 1 h at room temperature in the dark, and rinsed in cacodylate buffer (0.1 M, pH 7.4). The preparations were then dehydrated in graded ethanol solutions and embedded in Epon. Ultra-thin sections were cut with an ultramicrotome, contrasted with uranyl acetate and lead citrate, and examined under an H7500 electron microscope (Hitachi, Tokyo, Japan).

Immunofluorescence staining procedures, and antigen analysis by conventional fluorescence microscopy, laser scanning confocal microscopy, and flow cytometry

Immunofluorescence staining was performed on cells seeded at 10,000 cells/cm^2 on 12-mm glass coverslips. After 3 days of culture, cells were fixed with 2% paraformaldehyde for 5–15 min at room temperature or with 2.5% glutaraldehyde for 1 h at 4°C, washed with PBS, preincubated with FACS permeabilizing solution (BD-Biosciences) for 5 min at room temperature, and incubated with blocking buffer (PBS, 0.05% saponine (Sigma-Aldrich), 10% goat or bovine serum (PAN™ Biotech GmbH)) for 20 min at room temperature. After washing in PBS, cells were incubated for 1 h at room temperature with the following primary antibodies (mouse monoclonal antibodies raised against CNPase, catalase, used at 1/100; rabbit polyclonal antibodies directed against MBP, PLP, PMP70 (ABCD3), ACOX1 and L-PBE, and ALDP (ABCD1) used at 1/60, 1/200, 1/200, 1/100, 1/100, and 1/100, respectively;

a rat monoclonal antibody recognizing MOG used at 1/100) diluted in blocking buffer, washed in PBS, and then incubated for 30 min either with a 488-Alexa (or a 594-Alexa) goat anti-rabbit, anti-mouse or anti-rat used at 1/300. Nuclei were counterstained with Hoechst 33342 used at 2-µg/ml. After washing with PBS, slides were mounted, observations were made with an Axioskop Zeiss microscope, and digitalized images were obtained with an Axiocam Zeiss camera. To investigate the colocalization between mitochondria and PLP, cells were incubated with Mitotracker Red (100 nM, 15 min, 37°C), which stains mitochondria before the immunostaining procedure. Digital images acquisitions were collected with an SP2 AOBS confocal laser microscope (Leica) equipped for epifluorescence microscopy. Alexa488, Mitotracker Red, and Hoechst 33342 were excited with an argon ion laser, a Helium-Neon laser, and a blue diode, respectively. The objective magnification was x 40 with a 1.25 numerical aperture Plan Apochromatic oil immersion objective for high resolution (Lizard et al., 1994). Optical sections were obtained at 0.2 µm along the optical axis, and each plane consist of 1024 x 1024 pixels. Laser and diode powers, and detection gains were set up such that signals from single-stained controls would not appear in adjacent channels. The focal plane of maximal PLP expression within the cells was selected in order to maximize the probability of detection of colocalization with mitochondria (Santos et al., 2000). For colocalization of PLP and mitochondria, the ImageJ software was used.

For flow cytometric analyses, cells were collected by trypsinization (0.25% trypsin/EDTA solution) (Sigma), washed and mixed in PBS, and fixed in freshly prepared 2% (w/v) p-formaldehyde diluted in PBS (pH 7.4) for 10 min at room temperature. Furthermore, the cells were treated with the FACS permeabilizing solution 2 (BD-Biosciences) for 10 min. After washing in PBS, cells were incubated for 20 min with blocking buffer (PBS, 0.05% saponine, 10% goat serum), washed in PBS, and incubated for 1 h at room temperature with the appropriate primary antibody (mouse monoclonal antibodies raised against CNPase, catalase,

used at 1/100; rabbit polyclonal antibodies directed against MBP, PLP, PMP70, ACOX1, L-PBE, and ALDP used at 1/60, 1/200, 1/200, 1/100, 1/100, and 1/100, respectively; a rat monoclonal antibody recognizing MOG used at 1/100) diluted in blocking buffer. Then cells were washed twice with PBS and incubated for 1 h at room temperature either with a 488-Alexa goat anti-rabbit, mouse, or rat antibodies used at 1/300, 1/300 and 1/200, respectively. For the different secondary antibodies used, conjugated controls were performed. Cells were washed and mixed in PBS, and immediately analyzed by flow cytometry on a GALAXY flow cytometer (Partec). The green fluorescence of 488-Alexa was collected with a 520/10-nm band pass filter. The fluorescent signals were measured on a logarithmic scale. For each sample, 10,000 cells were acquired (dead cells and debris were excluded from the analysis by gating on living cells with the size/structure density plots), and the data were analyzed with FlowMax (Partec) and FlowJo (FlowJo Inc) softwares.

Protein extraction and Western blot analysis

Cells obtained after 3–4 days of culture were trypsinized (0.25% trypsin/EDTA solution), washed with PBS, and lysed in a RIPA buffer (Tris-HCl (0.05 M, pH 8), NaCl 0.15 M, SDS 0.1%, Na desoxycholate 0.5%, Nonidet®P40 1%, NaF 50 mM, EDTA 2 mM) in the presence of a complete protease inhibitor cocktail (Roche Diagnostics Inc) for 20 min on ice. Cell homogenates were cleared by 15 min centrifugation at 20,000 *g*. The supernatant was collected and used for gel electrophoresis associated with the immunoblot assay. The protein concentration of the samples was determined using the Bio-Rad DC protein assay kit (Ivry-sur-Seine, France), and bovine serum albumin (BSA) was used as standard. Forty micrograms of total protein extract were diluted in loading buffer 1X (Tris-HCl (125 mM, pH 6.8), 16% glycerol, 8% β-mercaptoethanol, 4% SDS and 0.003% bromophenol blue). Proteins were further separated by electrophoresis on a 10% polyacrylamide SDS-containing gel and

transferred onto a polyvinylidene difluoride membrane (Bio-Rad). After blocking nonspecific sites for 2 h with 5% skim milk and 1% BSA in Tris-buffered saline 1X (TBST: 10 mM Tris-HCl, 0.1% Tween 20, and 150 mM NaCl, pH 8), the membranes were incubated overnight at 4°C with various primary antibodies diluted in TBST, raised either against mice ALDP (1/300), ACOX1 (1/500), or L-PBE (1/200). After washing the membrane with TBST, it was incubated with horseradish peroxidase-conjugated anti-rabbit IgG (1/10,000) for 1 h at room temperature. The membranes were then washed with TBST and revealed using an enhanced chemiluminescence detection kit (Amersham) and autoradiography.

Enzymatic activities: ACOX1 and catalase

To perform enzymatic activity, the protein extract was prepared on 8–30 × 10^6 cells. Cells were mixed in 7.5 ml PBS containing a mixture of protease inhibitors (Roche Diagnostics Inc), and three successive freezing and thawing cycles were performed. The samples were sonicated, centrifuged (14,000 rpm, 30 min), and the supernatant was collected. ACOX1 activity was assayed by a fluorimetric assay as described by Oaxaca-Castillo et al. The reaction mixture (200 µl) contained Tris buffer (50 mM, pH 8.3), homovanillic acid (0.75 mM), horseradish peroxidase (20 µg/ml), and acyl-CoA substrate (palmitoyl-CoA at 50 µM final concentration). The reactions were started by the addition of 5–20 µl of enzymatic solution. Catalase activity was quantified with the Amplex Red Catalase Assay Kit (Invitrogen) which uses the highly fluorescent oxidation product, resorufin. The absorbance of resorufin-formed solution was measured at 570 nm using a spectrophotometer (Serlabo Technologies). One unit of the enzyme is defined as 1 µmol of H_2O_2 consumed per minute and the specific activity is reported as units per milligram of protein.

Quantitative RT-PCR

Cells were harvested with 0.25% trypsin/EDTA and washed with PBS. Total RNA from oligodendrocytes (158N or 158JP) was extracted using the RNeasy Mini kit (Qiagen) following the manufacturer's instructions. cDNA was generated by reverse transcription using QuantiTect Rev. Transcription Kit (Qiagen) according to the manufacturer's protocol and analyzed by quantitative PCR using the SYBR Green real-time PCR technology, and an iCycler iQ Real-Time Detection System (Bio-Rad). The primer sequences are: (*Abcd1:* forward 5'-acatccctatcatcacacccactg-3' and reverse 5'-gagaactcttgccacagccattg-3'; *Abcd2:* forward 5'-gttcaaagagaaggaggatgggatg-3' and reverse 5'-tgctcacggcactggtacattc-3', *Abcd3:* forward 5'-gctgggcgtgaaatgactagattg-3' and reverse 5'-ccttctcctgttgtgacaccattg-3', *Acox1:* forward 5'-gcccaactgtgacttccatt-3' and reverse 5'-ggcatgtaacccgtagcact-3'; *β-actin*: forward 5'-aacaccccagccatgtacg-3' and reverse 5'-atgtcacgcacgatttccc-3') were chosen using the Beacon Designer Software (Bio-Rad). PCR reactions were carried out in duplicate in a final volume of 25 µL containing 12.5 µL of MESA Green qPCR Mastermix (Eurogentec), 5 µL of cDNA and forward and reverse primers at 200 nM for *Abcd1*, 100 nM for *Abcd2*, or 300 nM for the other genes (*Abcd3*, *Acox1*, *β-actin*) studied. The PCR enzyme (*Taq* DNA polymerase) was heat-activated at 95°C for 10 min, and the DNA was amplified for 40 cycles at 95°C for 15 s, 60°C for 30 s, and 72°C for 30 s, followed by a melting curve analysis to control the absence of nonspecific products. For each transcript, the amplification efficiency was determined by the slope of the standard curve generated from two fold serial dilutions of cDNA. Gene expression was quantified using cycle to threshold (Ct) values and normalized by the *β-Actin* reference gene. The quantitative expression of *Abcd1*, *Abcd2*, *Abcd3*, and *Acox1* was determined according to $2^{-\Delta Ct}$ with ΔCt = (Ct of the gene studied) – (Ct of the *β-Actin* gene), or as fold induction of the control.

Flow cytometric characterization of mitochondrial and redox status

The mitochondrial potential ($\Delta\Psi m$) was measured with $DiOC_6(3)$ used at 40 nM (Miguet et al., 2001). The $DiOC_6(3)$-related green fluorescence was analyzed by flow cytometry and collected through a 520/10-nm band pass filter. The mitochondrial mass was studied with nonylacridine orange (NAO) (Ratinaud et al., 1988). To this end, cells mixed in PBS at 5×10^5 cells/ml were incubated for 30 min at 37°C with NAO used at 5 nM. After washing and mixing in PBS, cells were analyzed by flow cytometry, and the green fluorescence of NAO was collected through a 520/10-nm band pass filter. Both 2',7'dichlorodihydrofluorescein diacetate (H_2-DCFDA) and dihydroethidium (DHE) were used to characterize the production of reactive oxygen species (ROS) and of superoxide anions (O_2^-), respectively (Bass et al., 1983; Rothe and Valet, 1990). To measure the production of ROS, cells (10^6 cells/ml of culture medium) were incubated with H_2-DCFDA used at 6 µM final for 10 min at 37°C, and the green fluorescence of 2′,7′-dichlorofluorescein resulting from the oxidation of H_2-DCFDA was analyzed by flow cytometry and collected through a 520/10-nm band pass filter. DHE, a nonfluorescent compound rapidly oxidized in ethidium under the action of O_2^- (Rothe and Valet, 1990), was prepared at 10 mM in DMSO, and used at 2 µM on cell samples (10^6 cells/ml of culture medium). After 15 min of incubation at 37°C, cells were analyzed by flow cytometry. The red fluorescence of ethidium was collected through a 590/10-nm band pass filter.

The redox status was evaluated by the level of intracellular reduced glutathione (GSH) after staining with monochlorobimane (MCB) (Lizard et al., 1998). MCB, prepared at 4 mM, was added at 100–200 µM in cell suspensions (10^6 cells/ml in PBS). After 15 min of incubation at 37°C, cells were washed and mixed in PBS, and the blue fluorescence of MCB was collected with a 420-nm-long pass filter. The fluorescent signals were measured on a logarithmic scale on a GALAXY flow cytometer (Partec) equipped with an argon laser, and with a mercury

xenon lamp (to excite MCB). For each sample, 10,000 cells were acquired. The data were analyzed with FlowMax (Partec) and FlowJo (FlowJo Inc) softwares.

Statistical analysis

Statistical analyses were performed on at least three independent experiments using SigmaStat 2.03 software (Systat Software Inc) with the Mann-Whitney test, and data were considered statistically different at a *P*-value of 0.05 or less.

RESULTS

Analysis of oligodendrocytic and myelin markers using fluorescence microscopy and flow cytometry in 158N and 158JP cells

The expression of markers of differentiated oligodendrocytes (CNPase, MOG), and of major myelin proteins (PLP, MBP) was determined by fluorescence microscopy and flow cytometry. High levels of CNPase (Fig. 1A–C) and MOG (Fig. 1D–F) expression were observed. In agreement with previous investigations (Feutz et al., 2001; Ghandour et al., 2002), high levels of MBP (Fig. 1G–I) and PLP (Fig. 1J–L) expression were found. The expressions of CNPase, MOG, MBP, and PLP were either slightly or substantially higher in 158N than in 158JP cells.

Peroxisomal and mitochondrial content

Transmission electron microscopy was used to visualize peroxisomes in murine oligodendrocyte 158N and 158JP cells. Tissue sections from mice liver were used as positive controls (Fig. 2A-B). In 158N and 158JP cells, peroxisomes were also detected at the cytoplasmic level (Fig. 2C-F), but they were less numerous than in murine hepatocytes and had a heterogeneous aspect in the DAB reaction deposit. We also investigated the

morphological aspects of mitochondria in 158N and 158JP cells. Figure 2C-F shows clear morphological differences, in size and shape, between the mitochondria from 158N and 158JP cells. Indeed, the mitochondria from 158JP cells (Fig. 2F) were generally larger and more rod-shaped than the mitochondria of 158N cells (Fig. 2D). Thus, the consequences of PLP mutation and myelin synthesis disruption in the oligodendrocyte cell line 158JP might have a morphological impact on mitochondria shape.

Analysis of peroxisomal markers by fluorescence microscopy, flow cytometry, and Western blotting

The expression of the peroxisomal ABC transporters ALDP and PMP70 encoded by the *Abcd1* and *Abcd3* genes, respectively, and of the peroxisomal enzymes (catalase, ACOX1, L-PBE) was determined by fluorescence microscopy, flow cytometry, and Western blotting on 158N and 158JP cells. On these two cell lines, as shown by fluorescence microscopy and flow cytometry analyses, a high level of ALDP (Fig. 3A–C) and PMP70 (Fig. 3D–F) expression were observed. Substantial expression of catalase (Fig. 3G–I), ACOX1 (Fig. 3J–L), and L-PBE (Fig. 3M–O) were also detected. The expression of these peroxisomal markers was always higher in 158JP than in 158N cells. The expression of ALDP, ACOX1, and L-PBE was confirmed by Western blot analysis, which revealed the characteristic bands of these molecules (Fig. 3P). Thus, a major band at 75 kDa for ALDP, and an expected band at 78 kDa for L-PBE were identified (Suzuki et al., 1994; Fouquet et al., 1997) (Fig. 3P). The native 72-kDa ACOX1 protein is known to be cleaved inside the peroxisome mainly into a 50-kDa polypeptide protein (Oaxaca-Castillo et al., 2007). Using a polyclonal antibody, we detected the 72 and 50 kDa bands in 158N and 158JP cells, and these bands were not detected in the deficient ACOX1 fibroblasts (ACOX1 -/-) used as negative control (Fig. 3P).

Analysis of peroxisomal markers by RT-qPCR

The relative expression level of the *Abcd1*, *Abcd2*, *Abcd3*, and *ACOX1* genes was determined in 158N and 158JP murine oligodendrocytes by RT-qPCR and evaluated according to $2^{-\Delta Ct}$ calculated comparatively to β-actin (Fig. 4). Similar expression levels of *Abcd1* and *Acox1* were observed in 158N and 158JP cells, while the expression levels of *Abcd2* and *Abcd3* were higher in 158JP than in 158N cells. Moreover, *Abcd2* was very weakly expressed in 158N cells, whereas its expression level in 158JP cells was in the range observed for *Abcd1* and *Acox1*.

4-PBA responses of 158N and 158JP cells

4-PBA has been previously shown to induce peroxisomal genes and peroxisomal proliferation especially in rat hepatocytes (Gondcaille et al., 2005). It was therefore interesting to evaluate the response of 158N and 158JP cells to 4-PBA. Under treatment with 4-PBA (2.5 mM, 72 h), cell growth was strongly inhibited, and significant morphological changes were observed in both cell types (Fig. 5A–D). In 158N cells, the expression of the peroxisomal proteins ACOX1 and L-PBE was enhanced (Fig. 5E), as well as the expression of the myelin protein PLP (Fig. 5F) and the oligodendrocyte markers, MOG and CNPase (Fig. 5G). On 158JP cells, only a weak stimulation of the expression of CNPase was observed (Fig. 5E–G). As 4-PBA was shown to induce the transcription of *Abcd2* but not *Acox1* in glial cells (Condcaille et al., 2005), the expression levels of these genes was evaluated by RT-qPCR in both 4-PBA-treated or untreated 158N and 158JP cells. Data presented in supplementary file show that, in 158N cells, the mRNA levels of both *Abcd2* and *Acox1* was unchanged after 4-PBA treatment, while in 158JP cells 4-PBA induces slightly the mRNA level of *Acox1* and strongly the mRNA level of *Abcd2*.

In addition, specific activities of peroxisomal enzymes were also compared in untreated and in 4-PBA-treated 158N and 158JP cells. Whereas the catalase activity was similar in 158N and 158JP cells (Fig. 6A), ACOX1 activity was higher in 158JP than in 158N cells (Fig. 6B). In H4IIC3 rat hepatoma cells, used as positive controls, the catalase activity was approximately three times higher than in 158N and JP cells (data not shown). Thus, in both cell types, the 4-PBA treatments resulted in a significant increase in the activity of both enzymes (Fig. 6A-B). Observations made by transmission electron microscopy did not show a peroxisomal proliferation under treatment with 4-PBA in either 158N or 158JP, whereas an increase in the size of peroxisomes was found in 158N cells (data not shown).

Redox and mitochondrial status of 158N and 158JP cells

The oxidation of fatty acids requires both peroxisomal and mitochondrial activities, and the metabolic activities of these organelles are tightly connected to ensure the degradation of fatty acids contributing to produce acetyl-CoA. Therefore, the mitochondrial and redox status of murine oligodendrocytes of 158N and 158JP cells was investigated by flow cytometry with various dyes. The spontaneous production of ROS and of superoxide anions (O_2^-) measured by flow cytometry after staining with H_2-DCFDA and DHE, respectively, was significantly greater in 158JP than in 158N, as well as the intracellular level of reduced glutathione (GSH) quantified with MCB (Table 1). The mitochondrial potential ($\Delta\Psi m$), and the mitochondrial mass determined by flow cytometry after staining with $DiOC_6(3)$ and NAO, respectively, were also significantly higher in 158JP than in 158N cells. These data show substantial differences between the redox and the mitochondrial status of 158N and 158JP cells.

Confocal laser microscopic analysis of the interaction of PLP with mitochondria

Since 158JP cells express a mutated PLP form (Feutz et al., 2001) and since this protein could modulate the mitochondrial potential (Bongarzone et al., 2001) and contribute to the induction of a mitochondria-dependent form of cell death (Cerghet et al., 2001), we hypothesized that PLP could play a role in the differences in mitochondrial status observed between 158N and 158JP. Thus, by confocal laser scanning microscopy, after mitochondrial staining with Mitotracker Red and PLP identification by indirect immunofluorescence with Alexa 488, we studied the colocalization of PLP with mitochondria (Fig. 7). The number of colocalization sites of PLP with mitochondria were significantly ($P<0.05$) lower in 158N cells (2783 $\pm$ 4) (Fig. 7A-D), than in 158JP cells (9581 $\pm$ 23) (Fig. 7E-H), supporting the hypothesis that PLP, in addition to its role in myelination, might contribute to other cellular functions.

DISCUSSION

The central nervous system (CNS) comprises different cell types: neurons, microglial cells, and glial cells consisting of astrocytes, and oligodendrocytes. In the CNS, oligodendrocytes synthesize myelin made up of lipid (up to 70% dry weight) and two major proteins: the MBP and the PLP (Baumann and Pham-Dinh, 2001; Taylor et al., 2004). The myelin sheath of the CNS is formed by membranes that extend from oligodendrocytes and wrap concentrically around nerve fibres, thereby insulating them and facilitating rapid transmission of nerve impulses (Harauz et al., 2004). Myelin is a dynamic functionally active membrane, and its disruption due to intrinsic or environmental factors (Hörster et al, 2005; Eichler and van Haren, 2007) can result in serious neurological disorders including central and peripheral neuropathies (Zhou and Griffin, 2003), inflammatory demyelinating diseases such as multiple sclerosis (Steinman, 2008), and leukodystrophies such as Pelizaeus-Merzbacher disease, X-ALD, and P-NALD (Koeppen and Robitaille, 2002). Given that oligodendrocytes damage is observed in these different pathologies and that it has been demonstrated that oligodendrocytes play a crucial role in the progression of X-ALD (Kassman et al., 2007), it is important to develop cellular models since better knowledge of oligodendrocyte biology is crucial for the understanding of demyelination and remyelination mechanisms. To this end, murine or rat primary cultures of oligodendrocytes, as well as organotypic cultures can be used. However, these culture methods are difficult to standardize, and it may be advantageous to work on established oligodendrocyte cell lines. Consequently, we did an extensive characterization of the two murine oligodendrocyte cell lines 158N and 158JP isolated from the brain of normal and jimpy mice, respectively.

In agreement with previous investigations (Feutz et al., 2001; Ghandour et al., 2002), both cell lines strongly express the two major proteins of myelin, PLP and MBP, which account for 50% and 30% of whole myelin proteins, respectively (Taylor et al., 2004). In addition, these cells strongly express CNPase and MOG. CNPase is a myelin-associated enzyme localized

almost exclusively in the cells elaborating myelin (oligodendrocytes, Schwann cells), and it is involved in the growth of myelin membrane during early oligodendrocyte membrane biogenesis (Sprinkle, 1989). Whereas MOG only accounts for 0.1% of oligodendrocytic proteins, it is considered that this protein, which belongs to the immunoglobulin superfamily and plays important roles in the immune response associated with multiple sclerosis (Clements et al., 2003), could also contribute to the stability of myelin structure (Hörster et al., 2005). Thus, as 158N and 158JP cells express major proteins involved in the elaboration, the structure, and the immunoreactivity of myelin, they could be useful to study the effects of intrinsic and extrinsic factors on oligodendrocytic differentiation and study the role of the cellular metabolism in various pathologies associated with important myelin disorders such as the peroxisomal diseases X-ALD and P-NALD.

Several hypotheses have been postulated to explain the physiopathogenesis of the peroxisomal disorders, one of them presenting the toxicity of VLCFA for the myelin producing cells as central. So, it was important to characterize the peroxisomal equipment of the 158N and 158JP cells. Using transmission electron microscopy, some peroxisomes were detected in both cell lines, but they were less numerous than in mice hepatocytes. Interestingly, by using flow cytometry, western blotting, and/or RT-qPCR, we evidenced that 158N and 158JP express at a similar level the following peroxisomal markers: ALDP and PMP70 corresponding to the peroxisomal ABC transporters ABCD1 and ABCD3, respectively, as well as the peroxisomal enzymes catalase, ACOX1, and L-PBE.

Concerning X-ALD, several pharmacological compounds have been tested *in vitro* or *in vivo* to induce peroxisomal β-oxidation. One of them, 4-PBA, has been shown to induce the expression of *Abcd2* in mixed primary culture of murine oligodendrocytes and astrocytes (Gondcaille et al., 2005). It was therefore interesting to analyze the effect of 4-PBA on the 158N and 158JP cells. 4-PBA-treatments resulted in morphological changes concerning the

size and shapes of peroxisomes were only observed in 158N cells. Similarly, enhanced protein expression of ACOX1, L-PBE, PLP, MOG, and CNPase was also only observed in these oligodendrocytes isolated from normal mice, whereas CNPase was only slightly increased in 158JP cells. Although ACOX1 is induced by 4-PBA at both protein and enzymatic activity levels, no 4-PBA-effect has been detected for its mRNA. Thus, the ACOX1 expression in treated 158N cells could involve the existence of a post-translational up-regulation mechanism, which has been previously reported for other peroxisome proliferators (Hashimoto, 1987). Furthermore, it was also reported that 158JP cells have a defective cAMP metabolic pathway (Feutz et al., 2001). These observations, together with previous results showing that 158JP were unable to respond to basic fibroblast growth factor (bFGF) (Feutz et al., 1995) and dibutyryl cAMP (dbcAMP) (Feutz et al., 2001), suggest that 4-PBA-induced ACOX1, L-PBE, PLP, and MOG could occur in 158N through a cAMP-dependent pathway. On the other hand, since CNPase expression and catalase activity are enhanced by 4-PBA in both cell lines, our data support that these events could be independent of the cAMP pathway.

Surprisingly, in the absence of any treatment, ALDRP (ABCD2) gene was found poorly expressed in 158N cells as compared to 158JP cells, which harbour mutation in the PLP gene (Macklin et al., 1987). The increase of the basal expression of *Abcd2* gene in 158JP cells raises the question about the relationship between dysmyelination in JP mice oligodendrocytes and *Abcd2* gene regulation. Interestingly, PLP gene expression in oligodendrocytes was shown to be regulated via derepression mechanism involving several negative regulatory elements (Dobretsova and Wight, 1999). Accordingly, such repression/derepression mechanisms could explain the low level of Abcd2 mRNA in the myelinating 158N oligodendrocytes when compared to the strong induction of *Abcd2* mRNA level in 4-PBA-treated 158JP cells. Therefore, the use of both 158N and 158JP cell lines, instead of primary culture of murine oligodendrocytes, will be greatly helpful to depict the

regulation of *Abcd2* gene expression and the involved transcription factors, and to understand the substrate specificity of different peroxisomal ABC-transporters using gene silencing and/or gene transfection methods.

Peroxisomes and mitochondria are ubiquitous and tightly connected organelles, which have an indispensable role in the cellular metabolism of higher eukaryotes (Schumann and Subramani, 2008), and peroxisomal alterations can potentially influence mitochondrial functions (Hein et al., 2008; Fourcade et al., 2008). Consequently, given that peroxisomal and mitochondrial dysfunctions are often associated with neurological and developmental defects and that peroxisomes and mitochondria have been suggested to contribute to pathological conditions associated with oxidative stress (Schrader and Fahimi, 2006), the mitochondrial and the redox status were simultaneously studied in 158N and 158JP cells. Interestingly, significant differences were observed between 158N and 158JP cells: the spontaneous production of ROS and O_2^- was higher in 158JP than in 158N as well as the GSH level; $\Delta\Psi m$ and the whole mitochondrial mass were also higher in 158JP than in 158N. Although the primary causes of these differences are difficult to establish, it is tempting to speculate that the highest expression of mutated PLP observed in 158JP might be involved. This hypothesis is supported by the strong colocalization of PLP and mitochondria observed mainly in 158JP. Therefore, as previously suggested, in addition to its important role in myelin structure and functions, PLP might have additional roles (Campagnoni and Skoff, 2001). Indeed, potential roles of PLP in the induction of cell death have been suggested (Bongarzone et al., 2001), and it has been clearly established that increased levels of PLP favour the death of oligodendrocytes and neurons (Boucher et al., 2002; Skoff et al., 2004). Therefore, based on the data obtained in the present investigation and on those of the literature, we suggest that PLP could modulate the mitochondrial and the redox status, which subsequently could contribute to trigger cell death.

Our study shows that 158N and 158JP cells express the main proteins of mature oligodendrocytes (CNPase, MOG, and the two major proteins of myelin, PLP and MBP), contain major peroxisomal proteins and/or mRNAs (ALDP (ABCD1), PMP70 (ABCD3), catalase, ACOX1, L-PBE), and have different mitochondrial content and activities, and redox status. Interestingly, under treatment with 4-PBA, the expression of some of these proteins is enhanced, especially in 158N cells while *Abcd2* gene expression is only modulated in 158JP. Therefore, our data support that 158N and 158JP cells can provide powerful models to explore the relationships between peroxisome, mitochondrial metabolism, and myelin protein expression, and to dissect the complexity of the molecular mechanisms involved in some neurodegenerative diseases, especially X-ALD, P-NALD, and multiple sclerosis.

ACKNOWLEDGEMENTS

This work was supported by grants from the INSERM, CNRS, the council of Burgundy, the European Leukodystrophy Association (ELA), and the University Hospital of Dijon (CHU de Dijon).

REFERENCES

- Aubourg P, Dubois-Dalq M. 2000. X-linked adrenoleukodystrophy enigma: how does the ALD peroxisomal transporter mutation affect CNS glia? GLIA 29: 186-190.

- Bass DA, Parce JW, Dechatelet LR, Szejda P, Seeds MC, Thomas M. 1983. Flow cytometric studies of oxidative product formation by neutrophils : A graded response to membrane stimulation. J Immunol 130: 1910-1917.

- Baumann N, Pham-Dinh D. 2001. Biology of oligodendrocyte and myelin in the mammalian central nervous system. Physiol Rev 81: 871-927.

- Berger J, Gartner J. 2006. X-linked adrenoleukodystrophy: Clinical, biochemical and pathogenetic aspects. Biochim Biophys Acta 1763: 1721-1732.

- Bongarzone ER, Foster LM, Byravan S, Schonmann V, Campagnoni AT. 1997. Temperature-dependent regulation of PLP/DM20 and CNP gene expression in two conditionally-immortalized jimpy oligodendrocyte cell lines. Neurochem Res 22: 363-372.

- Bongarzone ER, Jacobs E, Schonmann V, Kampf K, Campagnoni CW, Campagnoni AT. 2001. Differential sensitivity in the survival of oligodendrocyte cell lines to overexpression of myelin proteolipid protein gene products. J Neurosci Res 65: 485-492.

- Boucher SE, Cypher MA, Carlock LR, Skoff RP. 2002. Proteolipid protein gene modulates viability and phenotype of neurons. J Neurosci 22: 1772-1783.

- Buntinx M, Vanderlocht J, Hellings N, Vandenabeele F, Lambrichts I, Raus J, Ameloot M, Stinissen P, Steels P. 2003. Characterization of three human oligodendroglial cell lines as a model to study oligodendrocyte injury: morphology and oligodendrocyte-specific gene expression. J Neurocytol 32: 25-38.

- Campagnoni AT, Skoff RP. 2001. The pathobiology of myelin mutants reveal novel biological functions of the MBP and PLP genes. Brain Pathol 11: 74-91.

- Cerghet M, Bessert DA, Nave KA, Skoff RP. 2001. Differential expression of apoptotic markers in jimpy and in Plp overexpressors: evidence for different apoptotic pathways. J Neurocytol 30: 841-855.

- Clements CS, Reid HH, Beddoe T, Tynan FE, Perugini MA, Johns TG, Bernard CC, Rossjohn J. 2003. The crystal structure of myelin oligodendrocyte glycoprotein, a key autoantigen in multiple sclerosis. Proc Natl Acad Sci U S A. 100: 11059-11064.

- Eichler F, van Haren K. 2007. Immune response in leukodystrophies. Pediatr Neurol 37: 235-244.

- Feutz AC, Bellomi I, Allinquant B, Schladenhaufen Y, Ghandour MS. 1995. Isolation and characterization of defective jimpy oligodendrocytes in culture. J Neurocytol 24: 865-877.

- Feutz AC, Pham-Dinh D, Allinquant B, Miehe M, Ghandour MS. 2001. An immortalized jimpy oligodendrocyte cell line: defects in cell cycle and cAMP pathway. Glia 34: 241-252.

- Forss-Petter S, Werner H, Berger J, Lassmann H, Molzer B, Schwab MH, Bernheimer H, Zimmermann F, Nave KA. 1997. Targeted inactivation of the X-linked adrenoleukodystrophy gene in mice. J Neurosci Res 50: 829-843.

- Fouquet F, Zhou JM, Ralston E, Murray K, Troalen F, Magal E, Robain O, Dubois-Dalcq M, Aubourg P. 1997. Expression of the adrenoleukodystrophy protein in the human and mouse central nervous system. Neurobiol Dis. 3: 271-285.

- Fourcade S, López-Erauskin J, Galino J, Duval C, Naudi A, Jove M, Kemp S, Villarroya F, Ferrer I, Pamplona R, Portero-Otin M, Pujol A. 2008. Early oxidative damage underlying neurodegeneration in X-adrenoleukodystrophy. Hum Mol Genet 17: 1762-1773.

- Ghandour S, Feutz AC, Jalabi W, Taleb O, Bessert D, Cypher M, Carlock L, Skoff RP. 2002. Trafficking of PLP/DM20 and cAMP signalling in immortalized jimpy oligodendrocytes. GLIA 40: 300-311.

- Gondcaille C, Depreter M, Fourcade S, Lecca MR, Leclercq S, Martin PG, Pineau T, Cadepond F, ElEtr M, Bertrand N, Beley A, Duclos S, De Craemer D, Roels F, Savary S, Bugaut M. 2005. Phenylbutyrate up-regulates the adrenoleukodystrophy-related gene as a nonclassical peroxisome proliferator. J Cell Biol 169: 93-104.

- Harauz G, Ishiyama N, Hill C, Bates IR, Libich DS, Farès C. 2004. Myelin basic protein-diverse conformational states of an intrinsically unstructured protein and its roles in myelin assembly and multiple sclerosis. Micron 35: 503-542.

- Hashimoto T. 1987. Comparison of enzymes of lipid β-oxidation in peroxisomes and mitochondria. In Peroxisome in Biology and Medicine. Fahimi DH and Sies H; eds; Springer-Verlag. Heidelberg. pp 97-105.

- Hein S, Schönfeld P, Kahlert S, Reiser G. 2008. Toxic effects of X-linked adrenoleukodystrophy-associated, very long chain fatty acids on glial cells and neurons from rat hippocampus in culture. Hum Mol Genet 17: 1750-1761.

- Hörster F, Surtees R, Hoffmann GF. 2005. Disorders of intermediary metabolism: toxic leukoencephalopathies. J Inherit Metab Dis 28: 345-356.

- Huin C, Schohn H, Hatier R, Bentejac M, Antunes L, Plénat F, Bugaut M, Dauça M. 2002. Expression of peroxisome proliferator-activated receptors alpha and gamma in differentiating human colon carcinoma Caco-2 cells. Biol Cell 94: 15-27.

- Hulshagen L, Krysko O, Bottelbergs A, Huyghe S, Klein R, Van Veldhoven PP, de Deyn PP, d'Hooge R, Hartmann D, Baes M. 2008. Absence of functional peroxisomes from mouse CNS causes dysmyelination and axon degeneration. J. Neurosci 28: 4015-4027.

- Jia Z, Pei Z, Li Y, Wei L, Smith KD, Watkins PA. 2004. X-linked adrenoleukodystrophy: role of very long-chain acyl-CoA synthetases. Mol Genet Metab 83: 117-127.

- Kassmann C, Lappe-Siefke C, Baes M, Brügger B, Mildner A, Werner HK, Natt O, Michaelis T, Prinz M, Frahm J, Nave KA. 2007. Axonal loss and neuroinflammation caused by peroxisome-deficient oligodendrocytes. Nat Genet 39: 969-976.

- Kemp S, Wanders RJ. 2007. X-linked adrenoleukodystrophy: Very long-chain fatty acid metabolism, ABC half-transporters and the complicated route to treatment. Mol Genet Metab 90:268-276.

- Kemp S, Wei HM, Lu JF, Braiterman LT, McGuinness MC, Moser AB, Watkins PA, Smith KD. 1998. Gene redundancy and pharmacological gene therapy: implications for X-linked adrenoleukodystrophy. Nat Med 4: 1261-1268.

- Koeppen AH, Robitaille Y. 2002. Pelizaeus-Merzbacher disease. J Neuropathol Exp Neurol 61:747-759.

- Lizard G, Chignol MC, Souchier S, Schmitt D, Chardonnet Y. 1998. Laser scanning confocal microscopy and quantitative microscopy with a chare coupled device camera improve detection of human papillomavirus DNA revealed by fluorescence in situ hybridization. Histochemistry 101: 303-310.

- Lizard G, Gueldry S, Sordet O, Monier S, Athias A, Miguet C, Bessede G, Lemaire S, Solary E, Gambert P. 1998. Glutathione is implied in the control of 7-ketocholesterol-induced apoptosis, which is associated with radical oxygen species production. FASEB J 12: 1651-1663.

- Macklin W, Gardinier M, King K, Kampf K. 1987. An AG→CG transition at a splice site in the myelin proteolipid protein gene in jimpy mice results in the removal of an exon. FEBS Lett 2: 417-421.

- Miguet C, Monier S, Bettaieb A, Athias A, Bessède G, Laubriet A, Lemaire S, Néel D, Gambert P, Lizard G. 2001. Ceramide generation occuring during 7β-hydroxycholesterol- and

7-ketocholesterol-induced apoptosis is caspase independent and is not required to trigger cell death. Cell Death Differ. 8**:** 83-99.

- Nguyen SD, Baes M, Van Veldhoven PP. 2008. Degradation of very long chain dicarboxylic polyunsaturated fatty acids in mouse hepatocytes, a peroxisomal process. Biochim Biophys Acta 1781: 400-405.

- Oaxaca-Castillo D, Andreoletti P, Vluggens A, Yu S, van Veldhoven PP, Reddy JK, Cherkaoui-Malki M. 2007. Biochemical characterization of two functional human liver acyl-CoA oxidase isoforms 1a and 1b encoded by a single gene. Biochem Biophys Res Commun 360: 314-319.

- Paintlia AS, Gilg AG, Khan M, Singh AK, Barbosa E, Singh I. 2003. Correlation of very long chain fatty acid accumulation and inflammatory disease progression in childhood X-ALD: implications for potential therapies. Neurobiol. Dis 14: 425-439.

- Poll-The BT, Roels F, Ogier H, Scotto J, Vamecq J, Schutgens RBH, Wanders RJA, van Roermund CWT, van Wiljand MJA, Schram AW, Tager JM, Saudubray JM. 1988. A new peroxisomal disorder with enlarged peroxisomes and a specific deficiency of acyl-CoA oxidase (pseudo-neonatal adrenoleukodystrophy). Am. J. Hum. Genet. 42: 422-434.

- Ratinaud MH, Leprat P, Julien R. 1988. In situ flow cytometric analysis of nonyl acridine orange-stained mitochondria from splenocytes. Cytometry 9: 206-212.

- Rothe G, Valet G. 1990. Flow cytometric analysis of respiratory burst activity in phagocytes with hydroethidine and 2',7'-dichlorofluorescin. J Leukoc Biol 47: 440-448.

- Santos MJ, Henderson SC, Moser AB, Moser HW, Lazarow PB. 2000. Peroxisomal ghosts are intracellular structures distinct from lysosomal compartments in Zellweger syndrome: a confocal laser scanning microscopy study. Biol Cell. 92: 85-94.

- Schrader M, Baumgart E, Völkl A, Fahimi HD. 1994. Heterogeneity of peroxisomes in human hepatoblastoma cell line HepG2. Evidence of distinct subpopulations. Eur J Cell Biol 64: 281-294.

- Schrader M, Fahimi HD. 2006. Peroxisomes and oxidative stress. Biochim Biophys Acta 1763: 1755-1766.

- Schrader M, Fahimi D. 2008. The peroxisome: still a mysterious organelle. Histochem Cell Biol 129: 421-440.

- Schumann U, Subramani S. 2008. Special delivery from mitochondria to peroxisomes. Trends Cell Biol 18: 253-256.

- Skoff RP, Bessert DA, Cerghet M, Franklin MJ, Rout UK, Nave KA, Carlock L, Ghandour MS, Armant DR. 2004. The myelin proteolipid protein gene modulates apoptosis in neural and non-neural tissues. Cell Death Differ 11: 1247-1257.

- Sprinkle TJ. 1989. 2',3'-cyclic nucleotide 3'-phosphodiesterase, an oligodendrocyte-Schwann cell and myelin-associated enzyme of the nervous system. Crit Rev Neurobiol 4: 235-301.

- Steinman L. 2008. Nuanced roles of cytokines in three major human brain disorders. J Clin Invest 118: 3557-3563.

- Suzuki Y, Shimozawa N, Yajima S, Tomatsu S, Kondo N, Nakada Y, Akaboshi S, Tanabe Y, Hashimoto T, Wanders RJA, Schutgens RBH, Moser HW, Orii T. 1994. Novel subtype of peroxisomal Acyl-CoA oxidase deficiency and bifunctional enzyme deficiency with detectable enzyme protein: identification by means of complementation analysis. Am J Hum Genet 54: 36-43.

- Taylor CM, Marta CB, Claycomb RJ, Han DK, Rasband MN, Coetzee T, Pfeiffer SE. 2004. Proteomic mapping provides powerful insights into functional myelin biology. Proc Natl Acad Sci U S A 101: 4643-4648.

- Verity AM, Bredesen D, Vonderscher C, Handeley VW, Campagnoni AT. 1993. Expression of myelin protein genes and other myelin components in an oligodendrocytic cell line conditionally immortalized with a temperature-sensitive retrovirus. J Neurochem 60**,** 577–587.

- Wanders RJ, Waterham HR. 2006a. Biochemistry of mammalian peroxisomes revisited. Annu Rev Biochem 75: 295-332

- Wanders RJ, Waterham HR. 2006b. Peroxisomal disorders : the single peroxisomal enzyme deficiencies. Biochim Biophys Acta 1763: 1707-1720..

- Zhou L, Griffin JW. 2003. Demyelinating neuropathies. Curr Opin Neurol 16: 307-313.

Table 1: Redox and mitochondrial status of murine oligodendrocytes 158N and 158JP

Assays	158N	158JP
ROS (H_2-DCFDA)	113.59 ± 25.09	170.20 ± 9.50 *
O_2^- **(DHE)**	2.83 ± 0.60	14.07 ± 0.92 ***
GSH (MCB)	13.80 ± 0.51	33.87 ± 2.01 ***
ΔΨm ($DiOC_6(3)$)	47.05 ± 10.50	122.60 ± 14.67 **
Mitochondrial mass (NAO)	34.44 ± 2.80	88.15 ± 9.57 ***

Data are expressed as ΔMFI (mean fluorescence intensity): ΔMFI = MFI of stained cells – MFI of unstained cells. Data are mean ± standard deviation of three independent experiments. Statistic significance of the differences between 158N and 158JP cells (* $P < 0.05$; ** $P < 0.005$, *** $P < 0.001$).

FIGURE LEGENDS

Figure 1: Expression analysis of oligodendrocytic and myelin markers in murine oligodendrocytes 158N and 158JP. Fluorescence microscopy and flow cytometry analysis were accomplished on subconfluent murine oligodendrocytes 158N and JP to determine the expression of oligodendrocyte differentiation markers such as 2',3' cyclic nucleotide 3'-phosphodiesterase (CNPase) (**A–C**), myelin oligodendrocyte glycoprotein (MOG) (**D–F**)), major myelin proteins (proteolipid protein (PLP) (**G–I**) and myelin basic protein (MBP) (**J–L**). Data shown are representative of three to six independent experiments. The scale bar is 10 µm. Control corresponds to conjugated control.

Figure 2: Transmission electron microscopy analysis of peroxisomes and mitochondria in murine oligodendrocytes 158N and 158JP. Livers of 9- to 10-week-old C57 Black/6 males were used as positive controls for peroxisome cytochemical analysis. **A**: Numerous peroxisomes (white arrows) are observed in a hepatocyte. **B**: These peroxisomes were clearly observed at high magnification in the presence of diaminobenzidine and H_2O_2. In 158N (**C, D**) and 158JP (**D, E**) cells, compared to murine hepatocytes, only a few peroxisomes were observed. Most often, the number of mitochondria (dark arrows) seems lower in 158N (**C**) than in 158JP (**E**). Data shown are representative of three independent experiments

Figure 3: Expression analysis of the peroxisome transporters and peroxisomal enzymes in murine oligodendrocytes 158N and 158JP. Conventional fluorescence microscopy and flow cytometry analyses were performed on subconfluent murine oligodendrocytes 158N and JP for peroxisomal transporters (ALDP (ABCD1) (**A–C**), and PMP70 (ABCD3) (**D–F**)) and for peroxisomal enzymes (catalase (**G–I**), acyl-CoA oxidase1 (ACOX1) (**J–L**), and peroxisomal bifunctional enzyme (L-PBE) (**M–O**)). ALDP, ACOX1, and L-PBE expression were also characterized using Western blotting (**P**). Data shown are representative of three to six independent experiments. The scale bar is 10 µm. Control corresponds to conjugated control. To investigate ACOX1 expression by Western blotting, we used homogenate from human fibroblasts deficient in ACOX1 (ACOX1 -/-).

Figure 4: Oligodendrocyte expression levels of genes encoding peroxisome transporters (Abcd1, Abcd2, Abcd3) or peroxisomal enzyme (Acox1) in murine oligodendrocytes 158N and 158JP, respectively. The mRNA levels were measured using real-time RT-qPCR and normalized to β-actin. Data presented are the mean ± standard deviation of two or three experiments (done in duplicate) and are expressed as $2^{-\Delta Ct}$.

Figure 5: Effect of 4-phenylbutyrate on the expression of peroxisomal proteins, and oligodendrocyte and myelin markers. (**A–D**) Phase-contrast microscopy showing untreated and 4-PBA (2.5 mM, 72 h) -treated 158N and 158JP cells. The scale bar is 30 µm. Flow cytometric analysis of the expression of peroxisomal proteins (PMP70, ACOX1, L-PBE) (**E**), major proteins of myelin (PLP, MBP) (**F**), and oligodendrocyte markers (CNPase, MOG) (**G**) on untreated and 4-PBA (2.5 mM, 72 h) -treated 158N and 158JP cells. Data shown are representative of two to three independent experiments. Control corresponds to conjugated control.

Figure 6: Effects of 4-phenylbutyrate on catalase and ACOX1 activities in murine oligodendrocytes 158N and 158JP. The activities of the peroxisomal enzymes (catalase (**A**) and ACOX1 (**B**)) were determined on subconfluent murine oligodendrocytes 158N and JP cultured in the absence or in the presence of 4-PBA used at 2.5 mM for 72 h. The enzymatic activities are expressed in fold induction comparatively to those of 158N cells used as reference. In these cells, catalase specific activity was 21.56 ± 2.99 µmol/min/mg of proteins, and ACOX1 specific activity was 6.00 ± 0.28 nmol/min/mg of proteins. Data shown are representative of two independent experiments done in triplicate. Results are presented as mean ± standard deviation; *, $P < 0.05$.

Figure 7: Analysis of the colocalization of PLP and mitochondria by confocal laser scanning microscopy. PLP was revealed with Alexa 488 and mitochondria were stained with Mitotracker Red. The nuclei were counterstained with Hoechst 33342. Overlay (C, G) was performed on optical sections showing the highest PLP-associated fluorescence (A, E) to maximize the probability of detection of PLP with mitochondria (B, F). The green dots correspond to colocalization sites (D, H). Interestingly, the number of green pixels are strongly higher in 158JP cells (9581 $\pm$ 23 green pixels / cell) (H) than in 158N cells (2783 $\pm$ 4 green pixels / cell) (D). The localization of PLP at the mitochondrial level was investigated with the colocalization finder plug-in of ImageJ software. For each slide observed, three microscopical fields were examined (four to six cells per field). Data shown are specific of three independent experiments. The scale bar is 10 µm.

<u>Supplementary file:</u> Effects of 4-phenylbutyrate on the expression levels of genes encoding for Abcd2 and Acox1 in murine oligodendrocytes 158N and 158JP. The mRNA levels were measured in control and 4-PBA (2.5 mM, 72 h)-treated 158N or 158JP cells. using real-time RT-qPCR and normalized to β-actin. Data presented are the mean ± standard deviation of three experiments (done in duplicate) and are expressed as fold induction of the control.

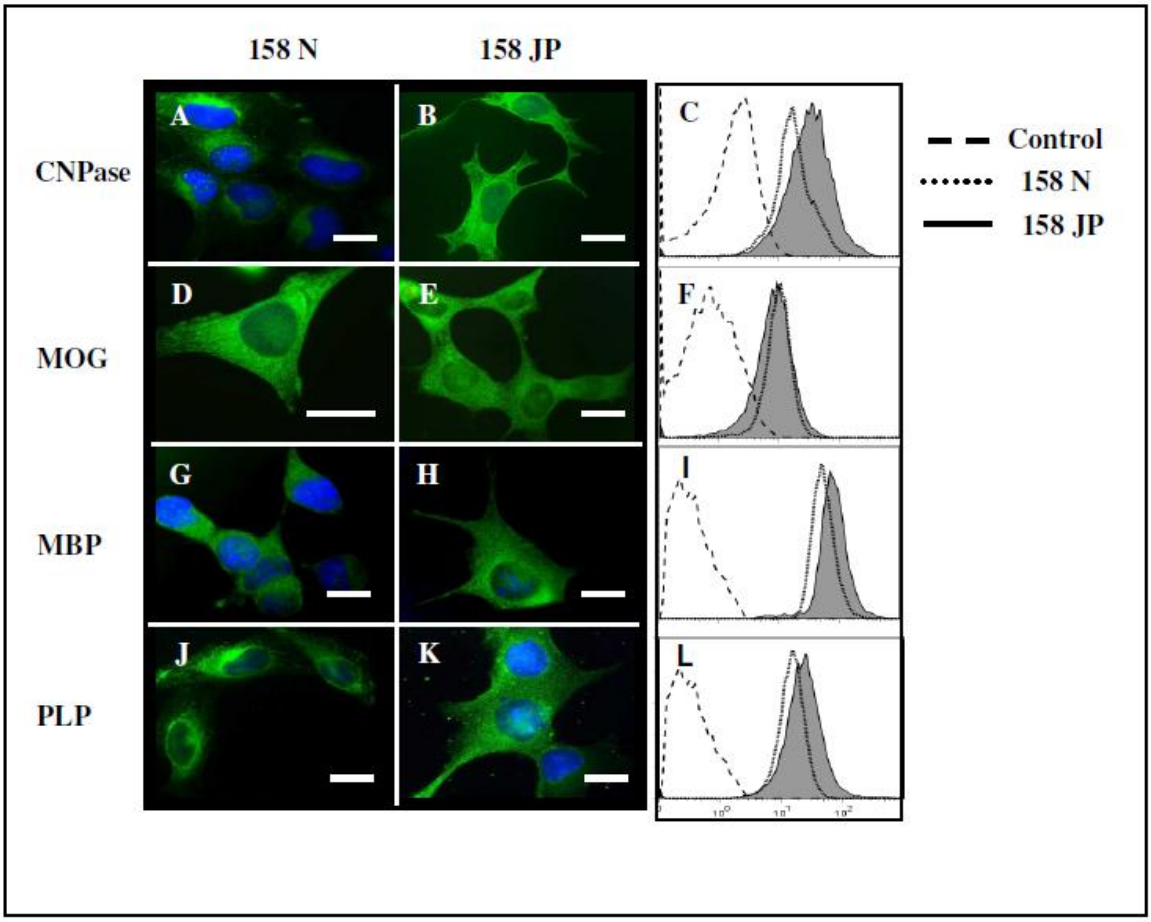
158 N
158 JP
CNPase
MOG
MBP
PLP
A
B
C
D
E
F
G
H
I
J
K
L
Control
158 N
158 JP

figure 1

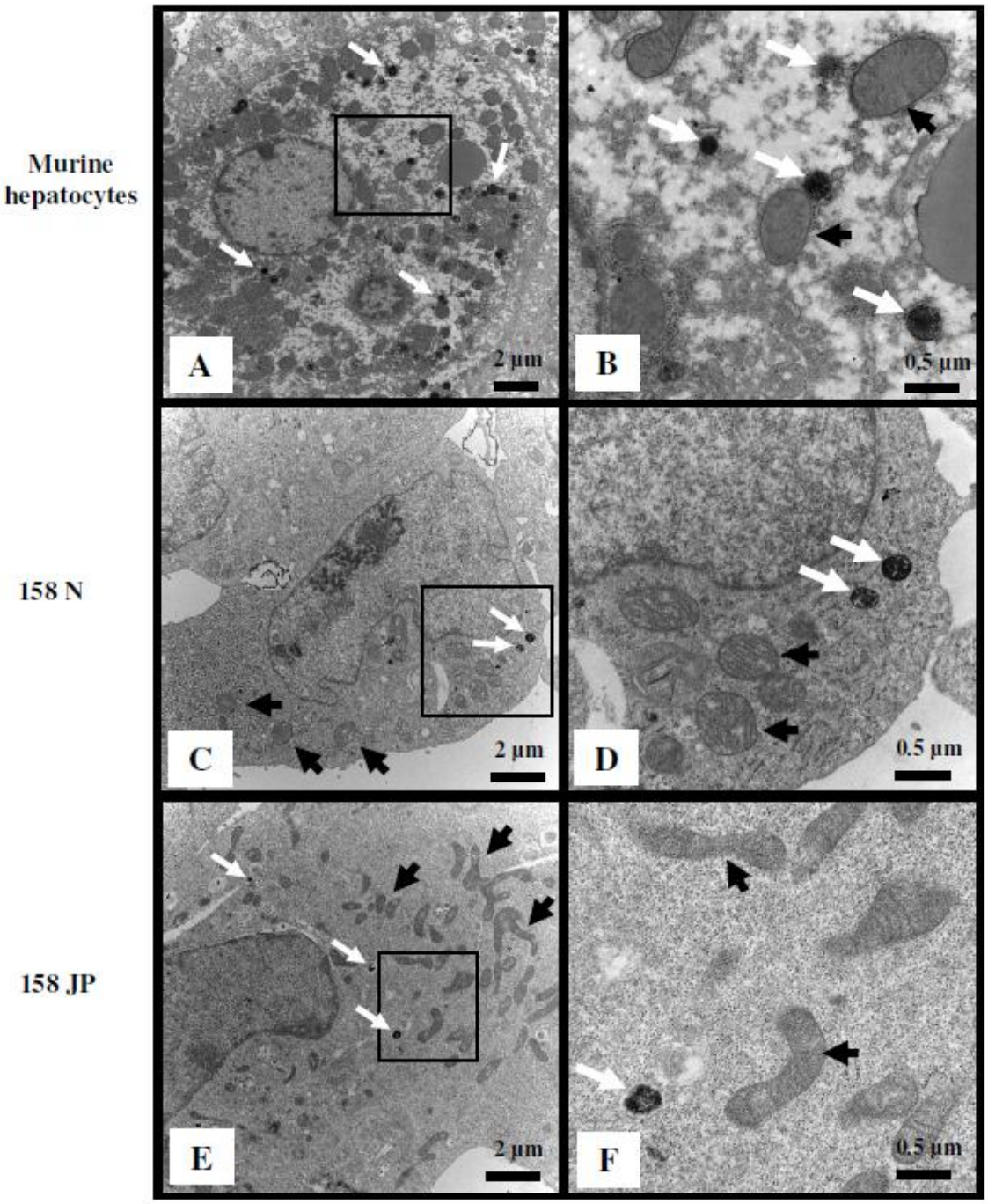
Murine hepatocytes
158 N
158 JP
A
2 µm
B
0.5 µm
C
2 µm
D
0.5 µm
E
2 µm
F
0.5 µm

figure 2

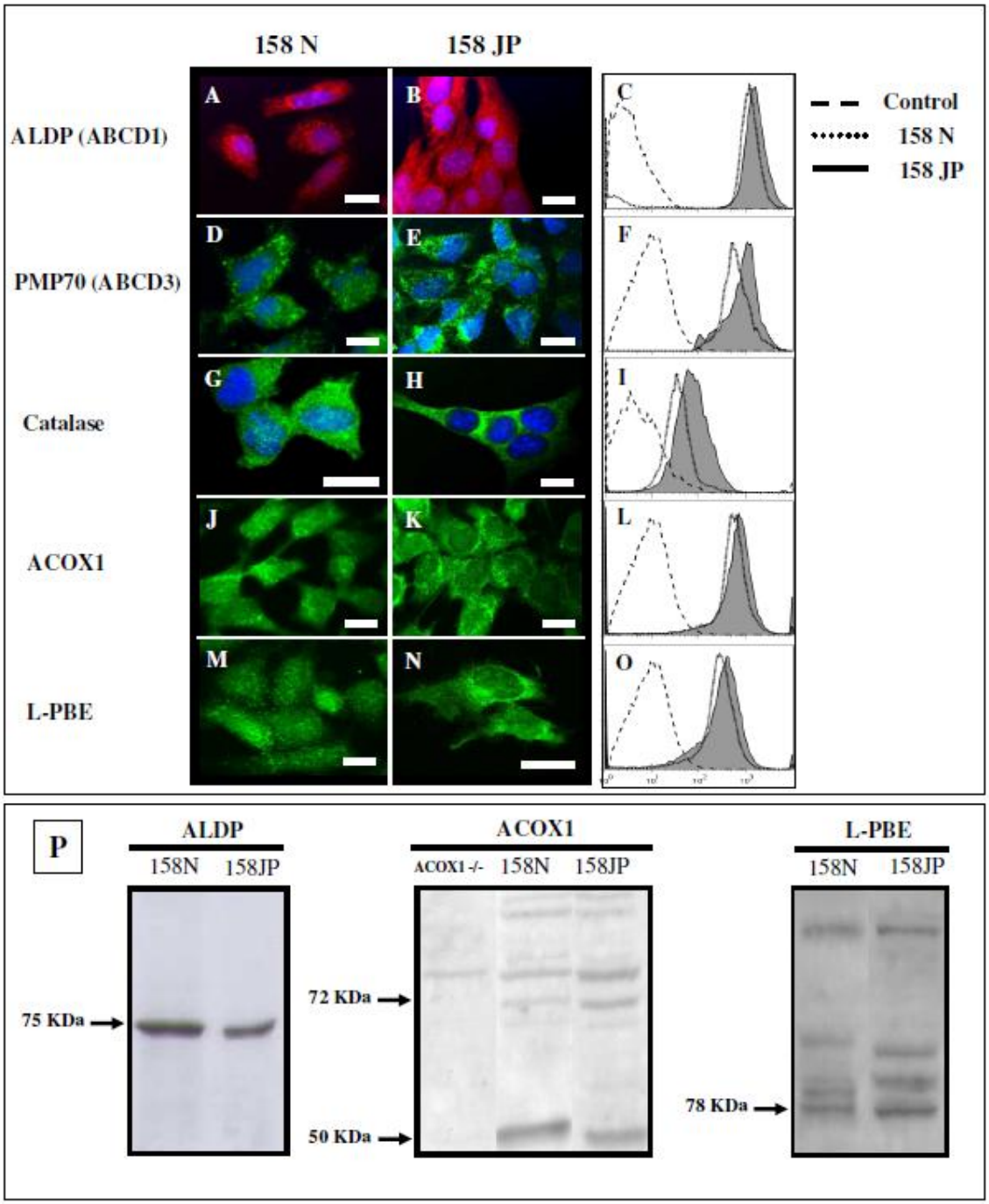
158 N
158 JP
ALDP (ABCD1)
PMP70 (ABCD3)
Catalase
ACOX1
L-PBE
A
B
C
D
E
F
G
H
I
J
K
L
M
N
O
Control
158 N
158 JP
P
ALDP
158N 158JP
75 KDa
ACOX1
ACOX1 -/- 158N 158JP
72 KDa
50 KDa
L-PBE
158N 158JP
78 KDa

figure 3

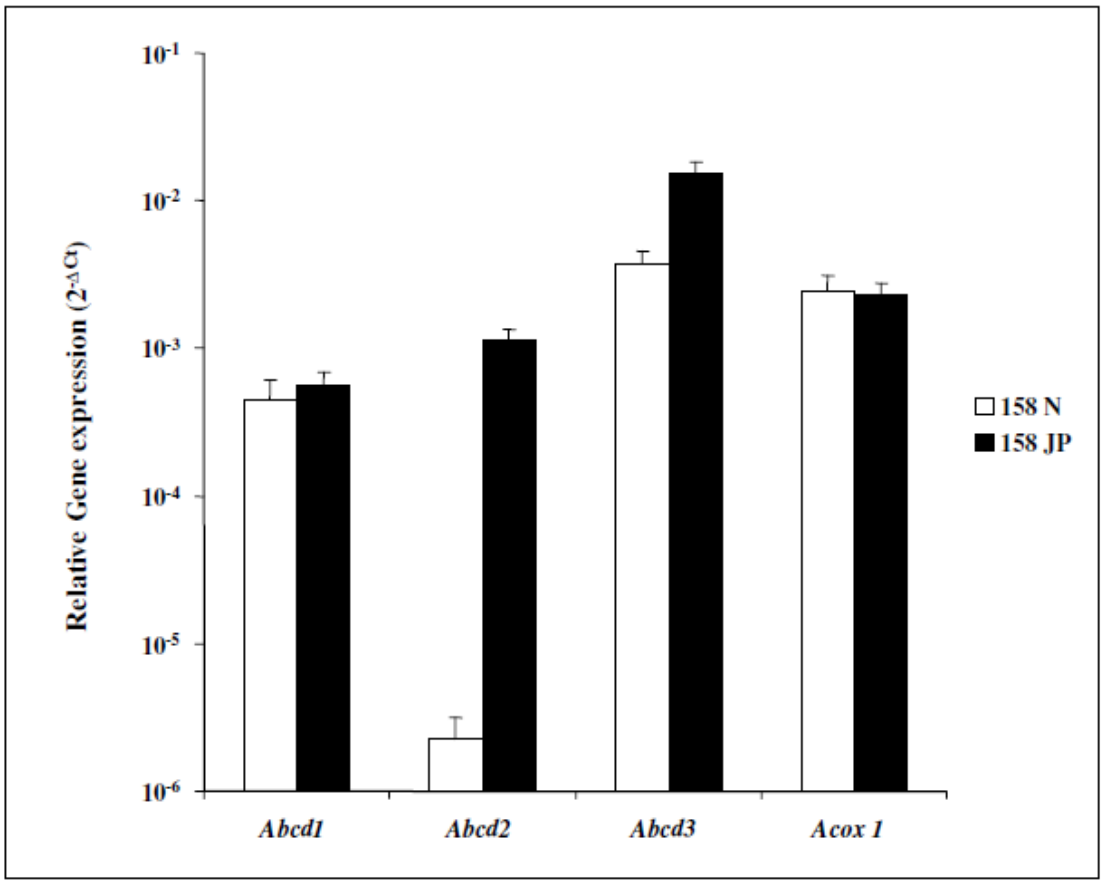
Relative Gene expression (2-ΔCt)
10-1
10-2
10-3
10-4
10-5
10-6
Abcd1
Abcd2
Abcd3
Acox 1
158 N
158 JP

figure 4

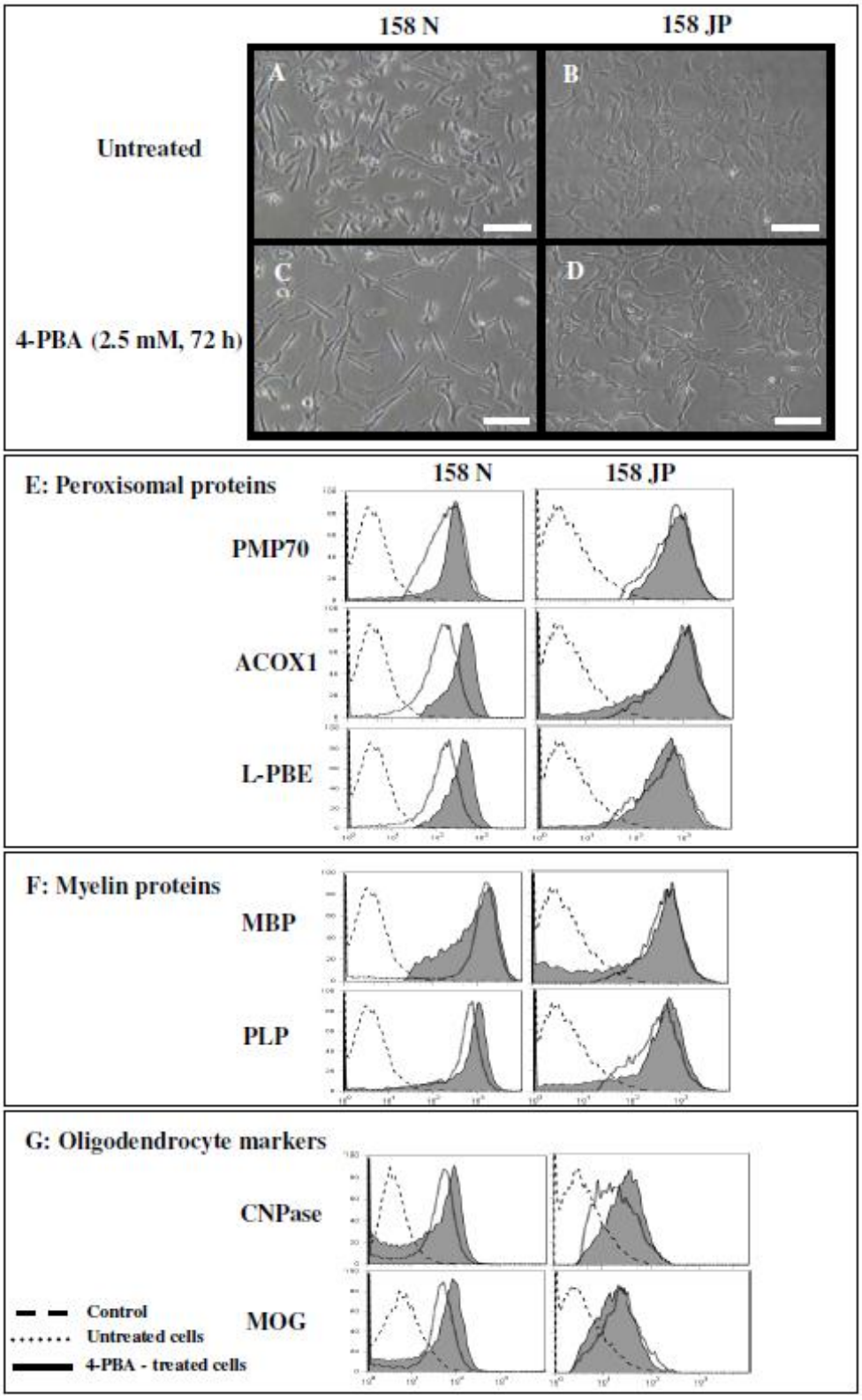
158 N
158 JP
Untreated
4-PBA (2.5 mM, 72 h)
A
B
C
D
E: Peroxisomal proteins
158 N
158 JP
PMP70
ACOX1
L-PBE
F: Myelin proteins
MBP
PLP
G: Oligodendrocyte markers
CNPase
MOG
Control
Untreated cells
4-PBA - treated cells

figure 5

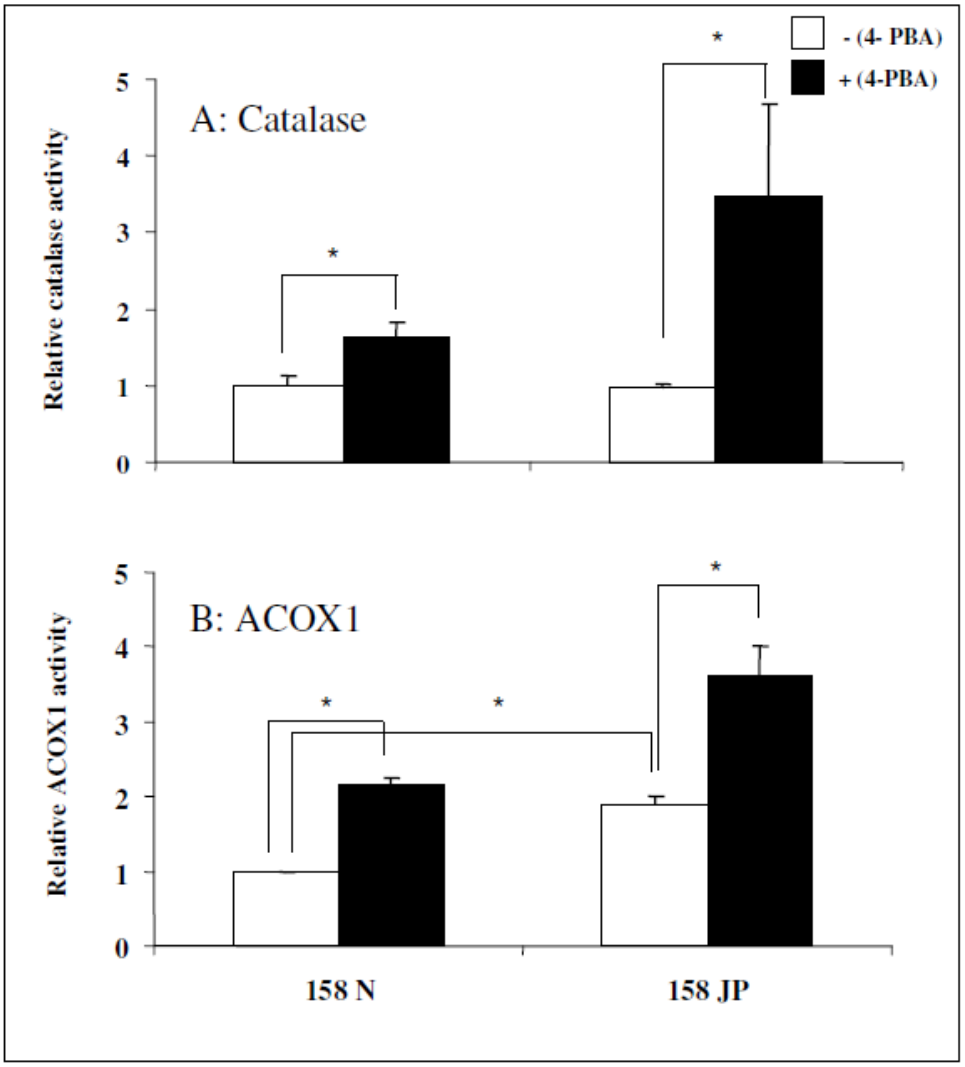
- (4- PBA)
+ (4-PBA)
A: Catalase
Relative catalase activity
B: ACOX1
Relative ACOX1 activity
158 N
158 JP

figure 6

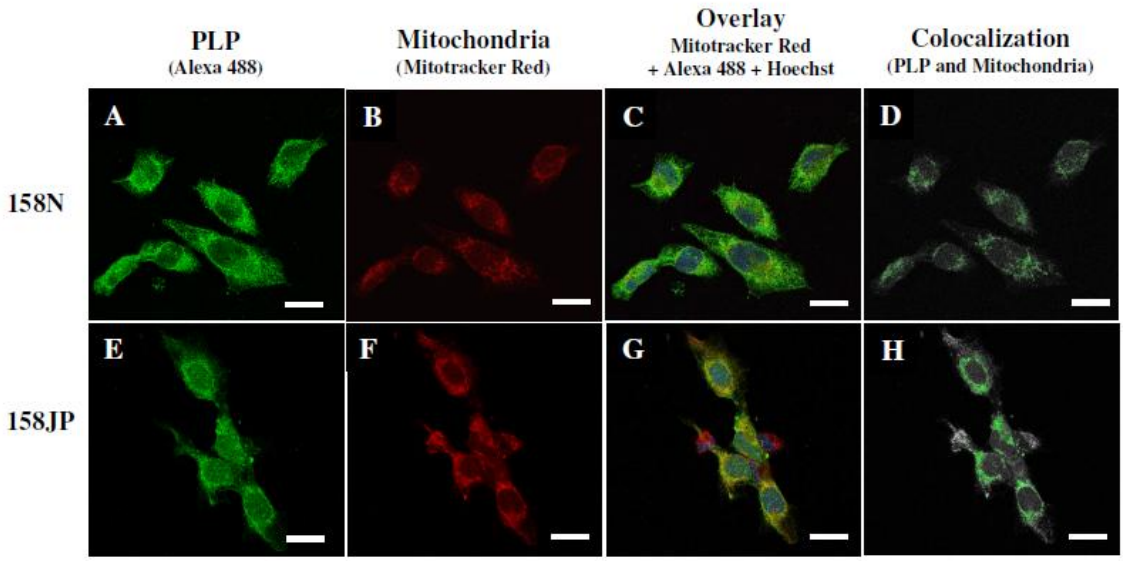
PLP
(Alexa 488)
Mitochondria
(Mitotracker Red)
Overlay
Mitotracker Red
+ Alexa 488 + Hoechst
Colocalization
(PLP and Mitochondria)
158N
158JP
A
B
C
D
E
F
G
H

figure 7